Journal of Environmental Management, Volume 389, August 2025, Article number 126133
DOI: 10.1016/j.jenvman.2025.126133

# Biochar Amendment and Water Level Optimization Enhance Nitrogen Removal and Reduce $N_2O$ Emissions in Vertical Flow Constructed Wetlands via metagenomic analysis

**Xin Wang[1], Zhiqiang Shen[1], Qin Zhang[1], Tao Lyu[2*], Yanli Ding[3], Shaoyuan Bai[1*]**

[1]*College of Environmental Science and Engineering, Guilin University of Technology, Guilin 541004, China*

[2]*Faculty of Engineering and Applied Sciences, Cranfield University, College Road, Cranfield, Bedfordshire MK43 0AL, United Kingdom*

[3]*College of Earth Sciences, Guilin University of Technology, Guilin 541004, China*

*Corresponding authors: baisy@glut.edu.cn (S. Bai), t.lyu@cranfield.ac.uk (T. Lyu)

## Abstract

To explore how biochar influences nitrogen cycling in unsaturated, capillary, and saturated zones of partially saturated vertical flow constructed wetlands (VFCWs), three parallel VFCWs were established to examine the effects of biochar's better water holding capacity on nitrogen removal and $N_2O$ emissions. Microbial mechanisms involved were studied by conducting ETS activity, metagenomic sequencing and performing high-throughput sequencing of 16S rRNA. Results indicated that the combination of adding 40% biochar and maintaining water level of 45cm facilitated TN removal and suppressed $N_2O$ emissions, achieving TN removal efficiency of 73.4% and $N_2O$/removed TN value of 0.3%. Within the unsaturated zone, the relative abundance of *amoA*, *hao*, and *nxrB* increased by 929%, 454%, and 38.3%, respectively, enhancing nitrification capacity microorganisms carrying these genes and involved in the oxidation of $NH_4^+$-N to $NO_3^-$-N included *Nitrosomonas, Methylosarcina, Nitrosospira, and Methylomonas*, whose relative abundance increased by 75.2%. In the capillary zone, the 19.2% increase in *nosZ* (involved in the reduction of $N_2O$ to $N_2$) transformed it into a potential $N_2O$ consumption layer. The functional genera involved in $N_2O$ reduction (*Ferrovibrio*, *Thauera*, *Ramlibacter*, and *Hyphomicrobium)* in the capillary zone increased by 1724%, 357%, 707%, and 78.5%, respectively, and the ETS activity in the 40W-CW capillary zone was 72.5% higher than that of QS-CW. Within the saturated zone, the relative abundance of *amoA* increased by 591%, *hao* by 149%, and *nxrB* decreased by 20.0%, potentially facilitating short-cut denitrification.

**Keywords**: Constructed wetland; $N_2O$; Biochar; Water level; Moisture; Water holding capacity

## 1. Introduction

Constructed wetlands (CWs), as nature-based solution, are extensively employed for the treatment of various wastewater and provide additional benefits, including biodiversity and carbon sequestration (Vymazal et al., 2018; Wang et al., 2023; Singh et al., 2024a). Because of the cost-effectiveness, high efficiency, low maintenance requirements, and minimal energy



Published by Elsevier. This is the Author Accepted Manuscript issued with: Creative Commons Attribution License (CC:BY 4.0).
The final published version (version of record) is available online at DOI:10.1016/j.jenvman.2025.126133. Please refer to any applicable publisher terms of use.

consumption, constructed wetlands have gained widespread adoption for decentralized and rural wastewater treatment (Singh et al., 2022; Soti et al., 2024). Vertical flow constructed wetlands (VFCWs), relying on natural hydraulic flow function without extra aeration energy input, exhibits excellent aerobic condition that could accelerate the oxidation of organics and $NH_4^+$-N compare with horizontal subsurface flow constructed wetlands (HSSFCW) and surface flow constructed wetlands (SFCWs) (Vymazal, 2013; Singh et al., 2024b). However, the high oxygen conversion capacity in VFCW limits the reduction of $NO_3^-$-N, resulting in a low total nitrogen (TN) removal efficiency (Wu et al., 2023).

The multistage CW flowsheet, equipping a HSSFCW or SFCW with more anoxic/anaerobic environment after the VFCW, could compensate for the insufficient denitrification capacity of VFCW and enable a significantly improved TN reduction. However, it will increase the requirement for land area (Vymazal, 2013). To further reduce the land demand and construction/operation costs, partially saturated VFCWs have been proposed to achieve TN removal because of its compatibility with anaerobic and aerobic environments (Zhao et al., 2013).

Water level is a crucial factor regulating the diffusion of oxygen in unsaturated zone, capillary zone and saturated zone, effectively changing the redox environment of VFCWs, consequently influencing the emission of $N_2O$ (Lu et al., 2019). Incomplete nitrification and incomplete denitrification are recognized as the primary contributors to the generation of $N_2O$ (Huang et al., 2023). On the one hand, insufficient dissolved oxygen (DO) in the bed during the process of nitrification inhibits the activity of nitrite oxidizing bacteria, resulting in the accumulation of $NO_2^-$-N (Huang et al., 2012). At this time, the microorganisms in the bed will express and form isomer nitrite reductase (iNxr), which utilises $NO_2^-$-N as electron acceptor to produce $N_2O$. On the other hand, the presence of oxygen in denitrification process impedes the conversion of $N_2O$ to $N_2$ as denitrifying bacteria prioritize the utilization of DO for respiration, resulting in the accumulation and emission of $N_2O$ (Foltz et al., 2019). Therefore, the height of the water level will significantly impact the configuration of the oxidation and reduction layer of VFCW. Regulation of water levels may optimize microbial community dynamics, thereby enhancing nitrogen removal efficiency and reducing $N_2O$ emissions. However, there are few reports on the relationship between water level and nitrogen cycling in partially saturated VFCW. Furthermore, the dynamics of functional gene expression under varying water levels have rarely been explored.

Biochar, a pyrolysis product of biomass waste, possesses a high specific surface area and porosity. The redox-active functional groups and persistent free radicals formed on its surface, such as quinone and hydroquinone moieties, facilitate electron transfer processes, enabling biochar to act as an electron shuttle and promote the balance between electron supply and demand within the system. The nitrogen transformation processes mediated by nitrogen-

cycling microorganisms are fundamentally driven by electron transfer mechanisms. In nitrification processes, electrons are transferred from ammonium to oxygen, facilitating ammonium oxidation while simultaneously providing both metabolic energy and reducing power for microbial activities. During denitrification, electrons are transferred from organic electron donors to nitrate, driving its sequential reduction to $N_2$ and consequently enabling effective nitrogen removal. Microbial communities establish sophisticated electron transfer networks through either direct intercellular connections or mediated electron transfer via electron shuttles, thereby facilitating synergistic nitrogen cycling processes. Notably, biochar serves as an efficient electron shuttle that significantly enhances interconversion between different nitrogen species through facilitated electron transfer, thereby optimizing the overall efficiency of nitrogen cycling. Additionally, the organic matter released from biochar can supplement carbon sources in the system, enhancing the activity of key enzymes and thereby reducing $N_2O$ emission (Zheng et al., 2022). Furthermore, biochar has also been found to improve the moisture retention and saturated hydraulic conductivity of substrate (Li et al., 2018; Wang et al., 2019). It facilitates the elevation of moisture, and affects the diffusion of $O_2$. Based on these advantageous properties, biochar has been widely applied in wastewater treatment and carbon emission reduction.

The biochar amendment in CWs is an important approach to enhance the treatment performance as well as reduce the greenhouse gas emission (Zhou et al., 2017). The addition of 20% biochar in the VFCW significantly improved the TN removal from 67% to 91% during the treatment of secondary wastewater effluent due to the enhanced enzymatic activity (Zheng et al., 2022). Similar results were also reported by Zhou in aerated VFCWs when treating simulated domestic sewage. However, there is controversy among previous researchers regarding whether biochar can inhibit the production of $N_2O$. Zhou et al. founded that attribute to the adsorption of biochar, and its ability to provide additional carbon sources, the application of biochar in VFCWs could reduce the emission of $N_2O$ by 271.29 - 554.59 $\mu g/(m^2 \cdot h)$ (Zhou et al., 2018). However, Huo et al. found that the biochar amendment stimulated the emission of $N_2O$ in VFCW (Huo et al., 2022). Banerjee's study showed that moisture is significantly positively correlated with $N_2O$ emission flux (Banerjee et al., 2016).

Biochar's better water holding capacity may play a pivotal role in influencing $N_2O$ emissions. However, few studies focus on the impact of biochar coupled with water level for simultaneous nitrogen removal enhancement and $N_2O$ emission reduction in partially saturated vertical flow constructed wetland. Metagenomics was employed to investigate the combined effects of biochar and water level on nitrification and denitrification pathways in constructed wetlands, identifying the abundance and expression levels of key functional genes and revealing the metabolic potential of microbial communities. The aim of this study is: 1) to investigate the combined effect of water level and biochar on TN removal capacity and $N_2O$ emission; 2) to reveal the nitrogen cycling processes in the unsaturated, capillary and

saturated zones of partially saturated VFCW filled with biochar; 3) to elucidate the key microbial mechanisms of biochar in reducing $N_2O$ emission.

## 2. Materials and Methods

### 2.1. Experimental setup and operation

Mesocosm-scale partially saturated VFCWs were established, with precipitation shielded (Fig. 1(a)). Each VFCW was made of polyvinyl chloride (PVC) column, with an inner diameter of 0.3 m and height of 1 m. The substrate comprises a 5cm diameter pebble bottom layer (0.15m) and a main medium layer (0.75m). Three parallel partially saturated VFCWs were named as follows: 1) QS-CW filled with quartz sand (Ø = 3 mm); 2) 20W-CW filled with a mixture of 20% wood biochar and 80% quartz sand; 3) 40W-CW filled with a mixture of 40% wood biochar and 60% quartz sand, respectively. The elemental composition of quartz sand and wood biochar is detailed in Table S1.

*Canna indica L.* was collected from local wetlands and planted at a density of three plants per VFCW. The wood biochar (Ø = 3 mm) was purchased from Zhengzhou Wantai Water Purification Materials Co., Ltd, Henan, China, which was prepared under carbonisation of raw materials under nitrogen flow at 500 °C.

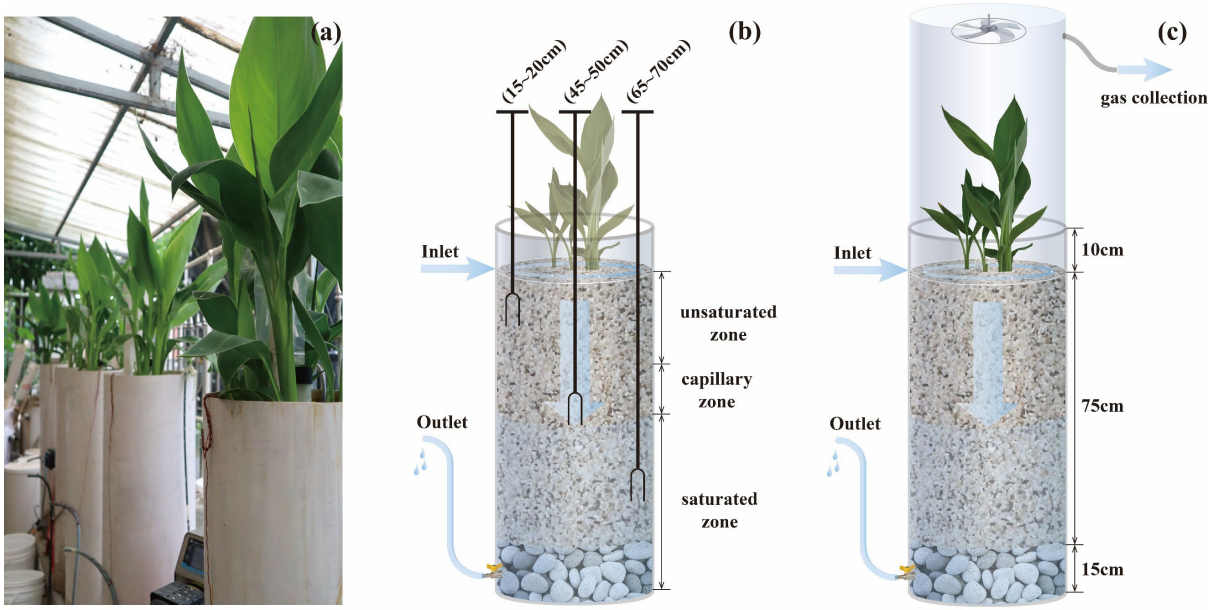



**Fig. 1.** The parallel VFCW experimental setup (a) the schematic diagram of the VFCW (b) with the $N_2O$ collection static chamber (c).

The experiment utilized campus domestic sewage as the influent for VFCW, which was controlled by a peristaltic pump to operate continuously in a downward flow within wetland. The hydraulic load rate (HLR) was maintained at 0.2 $m^3/(m^2 \cdot d)$, and the hydraulic retention time (HRT) was 24 hours correspondingly. The pollutant concentrations of influent are as follows: TN (54.7 ± 0.7 mg/L), $NH_4^+$-N (54.3 ± 2.8 mg/L), $NO_3^-$-N (0.2 ± 0.1 mg/L), COD (94.2 ± 3.2 mg/L), with DO and pH values of 1.6 ± 0.4 mg/L and 7.0 ± 0.04, respectively. The effluent

from VFCW was discharged through a hose connected to the bottom of the system (Fig. 1(c)), and the water level could be adjusted by modifying the hight of hose. Throughout the experiment, the water levels of VFCW were set at 35, 45, 55, and 65 cm, respectively. the system operated stably for one month under each water level condition, and the temperature during the experiment ranged from 16 and 25 $^{o}$C.

## 2.2. Sample collection and analysis

### *2.2.1. Water quality and Substrate moisture analysis*

The inlet and outlet samples were collected weekly to measure DO and pH values using a portable multi-parameter probe (HQ40D, Hach, USA). COD was determined by the dichromate method in accordance with the Chinese standard (HJ 808-2017). $NH_4^+$-N (HJ 535-2009), TN (HJ 636-2012), and $NO_3^-$-N (HJ/T 346-2007), were measured by UV spectrophotometer (UV-6100A, METASH, China). The quality of influents and effluents were presented in Table S3, Table S4, Table S5, and Table S6. The volumetric moisture (porosity) of each system was measured using Delta-T soil moisture sensors (PR2-6, Delta-T, UK) under varying water levels. The pore structure and surface morphology of the material was characterized by the scanning electron microscopy (SEM) and energy dispersive spectroscopy (EDS) (JSM-7900F, JEOL, Japan).

### *2.2.2. $N_2O$ collection and analysis*

Static chambers (Fig. 1(c)), equipped with a fan to mix air, were used to collect gas samples (Chen et al., 2020). The gas samples were collected at 0, 30, 60 and 120 min after the static chamber was closed between 9:00 am and 11:00 am and stored in the gas collection bag (200 mL, BKMAN, China). The collected gas samples were analysed using gas chromatograph (7890B, Agilent, USA) equipped with an electron capture detector (ECD). The $N_2O$ emission flux calculations followed the method reported by (Guo et al., 2020). The results of $N_2O$ emission were shown in Table S7, Table S8, Table S9 and Table S10.

## 2.3. microbial electron transfer system activity

Substrate samples of three different depth (15-20, 45-50, and 65-70 cm from the surface) were collected from each VFCW at a water level of 45 cm (Fig. 1(b)). The substrate samples were placed into 50 mL sterile plastic centrifuge tubes and stored in a -20 $^{o}$C refrigerator for microbial electron transfer system (ETS) activity, metagenomic sequencing and 16S rRNA high-throughput sequencing determination.

The 2-(p-iodophenyl)-3-(p-nitrophenyl)-5-phenyltetrazolium chloride-electron transport system (INT-ETS) method was employed to measure the activity of the ETS in microorganisms (Yin et al., 2018). The microbial ETS activity was determined using the Vicente method with slight modifications (Vicente et al., 2010). Briefly, 3 g of substrate samples were mixed with 10 mL Tris-Hcl buffer and sonicated in an ice bath for 4 minutes (0 $^{o}$C) to remove microorganisms on the surface of the substrate. The mixture was clarified and centrifuged at 4000 rpm for 5 minutes. Subsequently, 0.5 mL of supernatant and 1 mL of substrate solution (NADPH 0.25 mmol/L, NADH 1.7 mmol/L) were mixed with 0.5 mL INT. The mixture was incubated in an

incubator for 30 minutes, immediately after time incubation, the addition of 37% formaldehyde was carried out in order to stop the reaction. The absorbance of the sample at 490 nm was read with a spectrophotometer, the amount of $O_2$ consumed per unit time represents microbial ETS activity.

### 2.4 Metagenomic sequencing

The substrate samples were sent to Shanghai Sangon Biotechnology Co., Ltd. for metagenomic sequencing and 16S rRNA high-throughput sequencing.

The DNA extraction was conducted using the E.Z.N.A™ Mag-Bind Soil DNA Kit (OMEGA, USA), 1 % agarose gel electrophoresis was used to measure the integrity and purity of the DNA, and the concentration of the library was measured by Qubit 4.0 (ThermoFisher, USA). The Sequencing was conducted using the DNBSEQ-T7 platform (BGI, China). The metagenomic sequence data of substrate materials were mapped to the KEGG database (https://www.kegg.jp) for functional annotation. All raw sequencing data had been stored in the National Center for Biotechnology Information (NCBI) (Accession number: PRJNA1141715).

### 2.5 16S rRNA high-throughput sequencing

For the high-throughput sequencing, DNA samples were used as templates to amplify the V3-V4 hypervariable regions of the bacterial 16S rRNA gene with primer pairs 341F(CCTACGGGNGGCWGCAG) and 805R(GACTACHVGGGTATCTAATCC). Utilizing high-throughput sequencing of 16S rRNA, an in-depth analysis of active bacterial and microbial communities was conducted, with the diversity and relative abundance of metabolically active microorganisms enriched in the biofilm of constructed wetland substrates identified throughout the biological processes. 16S rRNA high-throughput sequence data had been stored in the National Center for Biotechnology Information (NCBI) (Accession number: PRJNA1195050).

### 2.6 Statistic analysis and visualization

SPSS 26.0 for windows (SPSS Inc., USA) was carried out for statistical analysis, the difference was considered significant only when $P < 0.05$. Corrplot package (v.0.92) in R 4.2.2 was implemented to analyse the correlation between water level and biochar addition on the performance of VFCWs.

## 3. Results and discussion

### 3.1. Impact of water level and biochar ratio

#### *3.1.1. Pollutants removal performance*

The impact of water level on pollutant purification on CWs was depicted in Fig. 2(a-d). With the HRT of 24h, the QS-CW exhibited the lowest efficacy in purifying pollutants. When the influent concentrations of COD, $NH_4^+$-N, TN and $NO_3^-$-N were 94.2 mg/L, 54.3 mg/L, 54.7 mg/L

and 0.2 mg/L respectively, the COD removal efficiencies at water levels of 35, 45, 55, and 65 cm were 52.7%, 68.8%, 29.9% and 51.4%, respectively. The corresponding $NH_4^+$-N removal efficiencies were 30.2%, 95.8%, 24.3% and 47.4%, respectively. $NH_4^+$-N was converted to $NO_3^-$-N, resulting in concentrations of 15.7 mg/L, 44.5 mg/L, 6.8 mg/L, and 14.1 mg/L, respectively. However, the TN removal efficiencies were only 5.1%, 5.7%, 5.5% and 12.6%, respectively, the low TN removal efficiency was primarily attributed to insufficient carbon sources, which inhibited the denitrification process.

Water level played a crucial role in regulating the diffusion of oxygen in VFCWs, subsequently affecting aerobic and anaerobic conditions, ultimately impacting the removal efficiency of pollutants. The purification of COD and $NH_4^+$-N were both oxidation processes, necessitating the involvement of DO. However, a persistent decline in water level did not continuously enhance oxidative conditions. This was particularly evident in the case of $NH_4^+$-N removal, where the QS-CW achieved the highest removal efficiency at water level of 45 cm. This phenomenon can be attributed to the insufficient contact between wastewater and microorganisms of unsaturated zone at lower water level, which may weaken the purification effect (Pelissari et al., 2018; Saeed et al., 2019).

Conversely, the TN removal efficiency of QS-CW increased with the rising water level, reaching a peak of 12.6% at water level of 65 cm. This indicated that an enlarged saturated zone favored the denitrification process in partially saturated VFCWs. Unlike $NH_4^+$-N and COD, the removal of TN predominantly occurs in the anoxic zone, where denitrifying bacteria facilitate the reduction of $NO_3^-$-N to $N_2$ through denitrification. Consequently, an elevated water level expands the anoxic zone, providing an enlarged habitat for denitrifying bacteria, thereby enhancing the denitrification process and ultimately improving TN removal efficiency. However, the increase in water level simultaneously reduces the volume of the unsaturated zone above the water level. Given that the aerobic degradation of COD and the aerobic nitrification of ammonia nitrogen primarily occur in the unsaturated zone, the reduction in its volume results in diminished removal efficiencies for both COD and $NH_4^+$-N when the water level is raised to 55 cm. It is noteworthy that as the water level in the QS-CW increased further from 55 cm to 65 cm, the removal efficiencies of TN, COD, and $NH_4^+$-N increased. This phenomenon can likely be attributed to the enhanced denitrification process driven by the elevated water level, as denitrification requires the consumption of organic carbon, leading to a concomitant reduction in COD concentration. Furthermore, the sustained anoxic conditions created by the higher water level may have facilitated the proliferation of specialized microbial communities, such as heterotrophic nitrifiers and short-cut nitrification-denitrification bacteria. These microorganisms possess unique metabolic pathways that enable them to utilize $NH_4^+$-N as a nitrogen source for growth and metabolism under low-oxygen or anoxic conditions, thereby promoting the nitrification of ammonia nitrogen and contributing to its improved removal efficiency (Hou et al., 2017; Zhang et al., 2018).

The addition of biochar significantly enhanced pollutant removal, and its effectiveness was notably influenced by water level. According to Fig. 2(a), all VFCWs demonstrated higher COD

removal efficiencies. COD removal efficiency at 35 cm water level in the 40W-CW was the highest (93.3%), representing an improvement of 49.7% compared to QS-CW ($P < 0.05$).

The influence of biochar on $NH_4^+$-N removal efficiency was strongly dependent on water level (Fig. 2(b)). At water level of 45 cm, the system achieved optimal performance, with the 20W-CW showing a mean removal efficiency of 94.1%, which was statistically comparable to that of QS-CW. When the water level was adjusted to 35 cm, the $NH_4^+$-N removal efficiency of 20W-CW increased by 39.4% ($P < 0.05$) compared to QS-CW, while the $NH_4^+$-N removal efficiency of 40W-CW increased by 35.3% ($P < 0.05$) compared to QS-CW.

As for $NO_3^-$-N and TN, biochar had a significant impact on the denitrification process. Before adding biochar, $NH_4^+$-N removal efficiency of QS-CW was 95.8%, the effluent concentration of $NO_3^-$-N was 44.5 mg/L, while the removal efficiency of TN was only 5.7% at water level of 45 cm, indicating that denitrification process was the primary factor limiting the overall removal of TN. After adding biochar, $NH_4^+$-N removal efficiency of 40W-CW was 90.1%, $NO_3^-$-N concentration decreased to 7.8 mg/L (Fig. 2(d)), the removal efficiency of TN increased to 73.4% (Fig. 2(c)) at water level of 45 cm, demonstrating that the denitrification ability of 40W-CW was significantly enhanced with biochar. Former studies indicate that this improvement can be attributed to biochar's ability to serve as both electron donor and electron shuttle, effectively facilitating the electron transfer process between microorganisms, promoting denitrification process and accelerating microbial degradation of pollutants (Cayuela et al., 2014; Saquing et al., 2016).

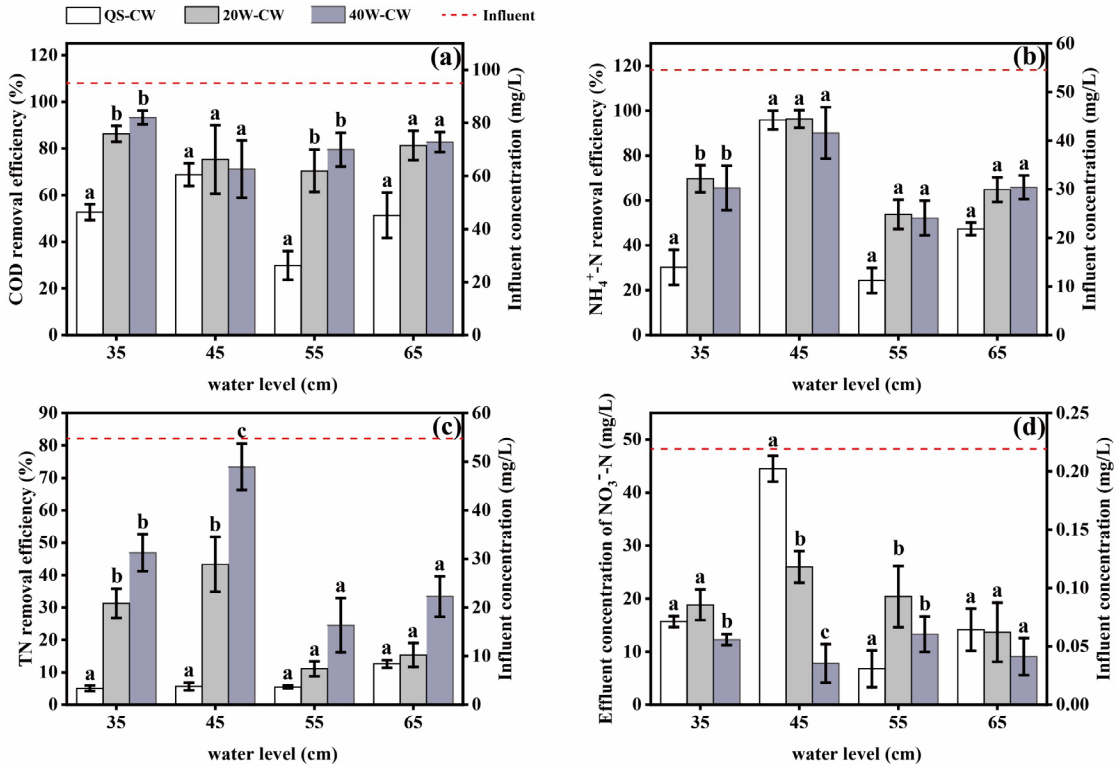



**Fig. 2.** The removal efficiency of COD (a), $NH_4^+$-N (b), TN (c) and $NO_3^-$-N (d) concentration of QS-CW, 20W-CW and 40W-CW at water levels of 35 cm, 45 cm, 55 cm 65 cm. Different lowercase letters represent the significant difference among VFCWs at $p < 0.05$ according to one-way ANOVA.

According to Liang's study, a higher biochar addition ratio enhanced nitrogen removal in CWs (Liang et al., 2020). The TN removal efficiency of 40W-CW was 37.7% and 67.8% higher than that of 20W-CW and QS-CW respectively, at the water level of 45 cm. However, the impact of the biochar addition ratio on COD and $NH_4^+$-N removal did not follow a consistent pattern, possibly due to the complex redox environment in VFCWs (Yang et al., 2018; Li et al., 2019; Guo et al., 2020). In addition to the influence of microbial processes, the adsorption of $NH_4^+$-N by biochar is also a key factor affecting nitrogen transformation in constructed wetlands. As shown in Fig. S2, the Langmuir isotherm model is more appropriate for characterizing the adsorption behavior of $NH_4^+$-N on biochar and quartz sand. The results demonstrated that biochar exhibited superior adsorption capacity for ammonium nitrogen ($K_L$ -biochar > $K_L$ -quartz sand), with a maximum adsorption capacity ($q_{max}$) of up to 3400.09 mg/kg (Table S2). These findings indicate that direct adsorption by biochar is one of the factors determining nitrogen transformation processes. Moreover, enhanced adsorption capacity ensures a more extensive and consistent nutrient supply for the microbial communities.

Based on the experimental results, a mismatch between water level variations and denitrification processes was observed. Three potential reasons were summarized: (1) Redox condition alteration: Variations in water level significantly modify the redox conditions within the substrate, which indirectly influences microbial-driven nitrogen transformation processes. Higher water levels tend to create more extensive anaerobic zones, favoring denitrification but potentially limiting nitrification due to reduced oxygen availability;

(2) Microbial-wastewater interaction: Fluctuations in water level affect the contact between wastewater and microorganisms, thereby influencing the microbial consumption of $NH_4^+$-N and COD. Enhanced contact under certain water levels may promote microbial activity, while excessive water levels could restrict oxygen diffusion, negatively impacting aerobic processes;

(3) Substrate adsorption capacity: The adsorption capacity of the substrate for $NH_4^+$-N and COD is influenced by the interaction between wastewater and substrate materials. Although rising water levels weaken oxygen transfer, they may also enhance the contact between wastewater and substrate, creating more favorable conditions for the direct adsorption of ammonium nitrogen and its subsequent microbial consumption.

Although elevated water levels can attenuate oxygen transfer efficiency in constructed wetlands, they may concurrently enhance the interfacial interaction between wastewater and substrate materials. This intensified contact could establish more conducive conditions for the direct adsorption of NH4$^+$-N and its subsequent microbial assimilation, thereby facilitating nitrogen removal processes. Comparing the results of the four water levels, VFCWs exhibited the highest removal efficiencies at water level of 45 cm, with the 40W-CW achieving a notable TN removal efficiency of 73.4%.

### *3.1.2. $N_2O$ emission*

As shown in Fig. 3, $N_2O$ fluxes of QS-CW were 0.2 mg/($m^2$·h), 0.8 mg/($m^2$·h), 0.2 mg/($m^2$·h) and 0.7 mg/($m^2$·h) at water levels of 35 cm, 45 cm, 55 cm and 65 cm, respectively. Furthermore, significant differences ($P < 0.05$) were observed in $N_2O$ fluxes across the four water levels. For biochar-VFCWs, the $N_2O$ fluxes of 20W-CW were 0.6 mg/($m^2$·h), 1.0 mg/($m^2$·h), 0.6 mg/($m^2$·h) and 0.9 mg/($m^2$·h), respectively. Similarly, the $N_2O$ fluxes of 40W-CW were 0.4 mg/($m^2$·h), 0.8 mg/($m^2$·h), 0.5 mg/($m^2$·h) and 0.4 mg/($m^2$·h) at water levels of 35 cm, 45 cm, 55 cm 65 cm, respectively.

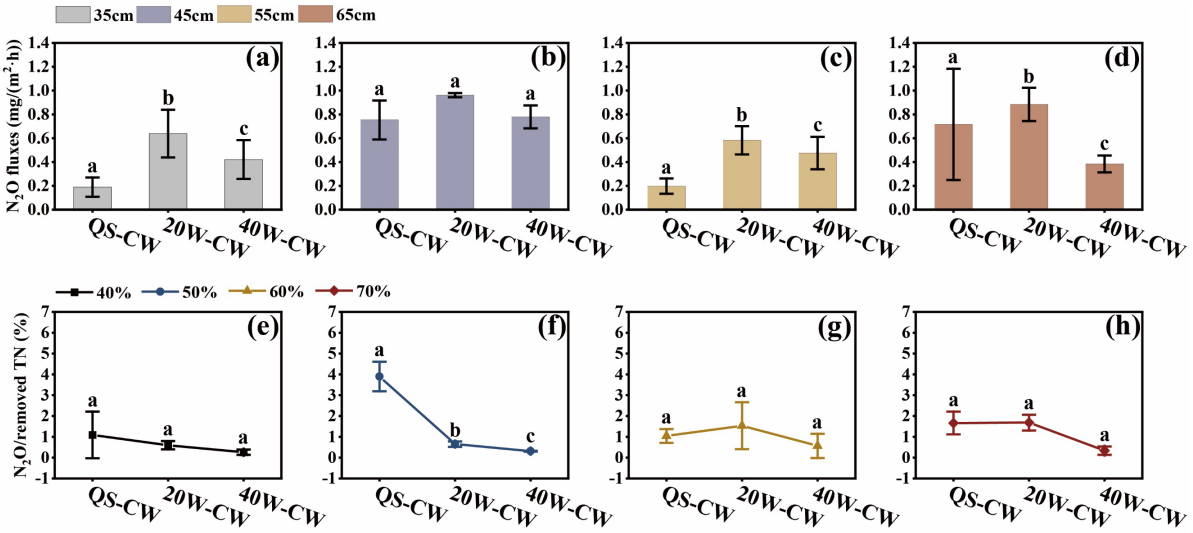



**Fig. 3.** $N_2O$ emission fluxes of VFCWs at water levels of 35 cm (a), 45 cm (b), 55 cm (c) and 65 cm (d). And $N_2O$/removed TN of VFCWs (quartz sand, 20% and 40% biochar) at water levels of 35 cm (e), 45 cm (f), 55 cm (g) and 65 cm (h), respectively. Different lowercase letters represent the significant difference among VFCWs at $p < 0.05$ according to one-way ANOVA.

According to $N_2O$ fluxes, biochar promoted the emission of $N_2O$, consistent with the findings of Huo and Feng (Feng et al., 2020; Huo et al., 2022) . Water level was important in influencing $N_2O$ fluxes, with the maximum $N_2O$ emission observed at water level of 45 cm. This was attributed to the higher $NH_4^+$-N and TN removal efficiencies (Fig. 2(bc)), which accelerated the nitrogen cycling process and $N_2O$ emission.

It was investigated that $N_2O$/removed TN value represented the proportion of $N_2O$ emissions, making it a more reasonable metric when compared to $N_2O$ flux alone (Huo et al., 2022). The $N_2O$/removed TN values were shown in Fig. 3. The $N_2O$ flux of QS-CW was the highest at a water level of 45 cm (0.8 mg/($m^2$·h)), and correspondingly, the $N_2O$/removed TN value was also at its highest (3.9%). As the water level rose from 45 cm to 55 cm and 65 cm, the $N_2O$/removed TN values of QS-CW declined to 1.1% and 1.7%, respectively. This reduction may be attributed to the increase in the saturated zone, which enhanced denitrification and helped suppress the emission of $N_2O$ during denitrification. Fig. 2(c) indicated that TN removal efficiency in QS-CW increased with the water level, accompanied by a decrease in $NO_3^-$-N concentration.

For biochar- VFCWs, the $N_2O$/TN removal remained stable at water levels of 35 cm and 45 cm. Specifically, the $N_2O$/TN removal values were 0.6% - 0.7% for 20W-CW and 0.3% for 40W-CW. The $N_2O$/removed TN increased as the water level rose to 55 cm and 65 cm . For 20W-CW, the $N_2O$/removed TN value reached 1.7% at water level of 65 cm, representing a 182% increase compared to ratio at water level of 35 cm. Meanwhile, the $N_2O$/removed TN ratio of 40W-CW remained at 0.3% at water level of 65 cm. Compared with 20W-CW, the mean $N_2O$/removed TN value of 40W-CW decreased by 66.9%, suggesting that increasing the proportion of biochar may be beneficial for reducing both $N_2O$ flux and $N_2O$/removed TN values.

However, as shown in Fig. 2(b), the increase in water level resulted in lower $NH_4^+$-N removals. Consequently, it was speculated that the increase in $N_2O$/removed TN at water level of 55 cm and 65 cm was caused by inefficient nitrogen cycling processes. These findings indicated that controlling the water level in partially saturated VFCWs was a prerequisite for ensuring nitrogen removal efficiency. On this basis, the addition of biochar can effectively reduce $N_2O$ emission. At water level of 45 cm, 40W-CW achieved both the highest TN removal efficiency and the lowest $N_2O$/removed TN, representing optimal performance conditions.

### 3.2 Substrate moisture

Based on the variation of moisture across different gradients, VFCWs were divided into 3 layers, including the saturated zone (below the water level), the capillary zone (10 cm above the water level with a sharp change in moisture), and the unsaturated zone (above the capillary zone). The moisture volume and air volume of the substrate generally exhibited a negative correlation in the unsaturated zone and capillary zone. As the moisture increased, the air volume within the substrate decreased, leading to an increase in the resistance to oxygen diffusion.

As illustrated in Fig. 3, the enhanced water-holding capacity of biochar significantly increased the moisture of the wetland bed ($P < 0.05$), indicating that the moisture of VFCWs rose with the addition of biochar. Specifically, compared to QS-CW (0% biochar), the moisture of 20W-CW (20% biochar) and 40W-CW (40% biochar) increased by 9.7% and 14.5%, respectively, at water level of 45 cm.

Furthermore, an elevation in water level resulted in a corresponding increase in moisture. Among these three VFCWs, as the water level increased, the moisture in the unsaturated zone gradually increased, followed by a sharp increase in the capillary zone. In QS-CW, the mean moisture in the unsaturated zone was 7.1%, 7.7%, 6.7%, and 7.9%, respectively, while the mean moisture in the capillary zone exhibited a significant increase, reaching 12.1%, 11.8%, 17.7%, and 25.5%, respectively. This phenomenon occurred because the moisture distribution in partially saturated VFCWs was influenced by the capillary force between the wastewater and substrate pores in the unsaturated zone, which led to a notable change in moisture above the water level (Yao et al., 2019). Furthermore, a clear boundary existed between the unsaturated zone, capillary zone and saturated zone. The capillary zone served as a

transitional zone that separated the air within the substrate.

The mean moisture in the capillary zone of QS-CW, 20W-CW, and 40W-CW at water level of 45 cm were 11.8%, 20.6%, and 63.4%, respectively (Fig. 4(b)). The addition of 20% and 40% biochar further promoted the moisture in capillary zone ($P < 0.05$). It has been reported that the moisture retention capacity of biochar is mainly determined by its hydrophilicity and porous structure (Wang et al., 2019; Yi et al., 2020; Edeh et al., 2021). As shown in Fig. 2 and Fig. 3, the elevated moisture of 40W-CW not only improved the efficiency of TN removal but also contributed to a reduction in $N_2O$/ removed TN. This effect could be attributed to the enhanced denitrification performance of 40W-CW. It was speculated that the high moisture restricted the diffusion of $O_2$, thereby expanding the denitrification zone and enhancing the nitrogen removal capacity of 40W-CW (Mekala et al., 2017). When the water level increased to 65 cm, the constructed wetland exhibited higher moisture content. However, the TN removal efficiency declined (Fig. 2(c)). Analysis of ammonium and nitrate nitrogen dynamics revealed that as the water level increased, the volume of the unsaturated zone above the water level diminished, thereby reducing the habitat available for nitrifying bacteria. This resulted in a decrease in $NH_4^+$-N removal efficiency. Consequently, less $NO_3^-$-N was transported from the nitrification zone into the capillary fringe and the submerged denitrification zone below the water level, while more $NH_4^+$-N accumulated. Thus, although the 40W-CW system provided suitable conditions for denitrification, the TN removal efficiency was compromised due to the insufficient availability of $NO_3^-$-N.

Fig. 4(e) represented the relationship between moisture, nutrient removal, and $N_2O$ emission in QS-CW. The results suggested a significant positive correlation between moisture and water level ($P < 0.05$), emphasizing water level as a key factor in increasing moisture. The $NH_4^+$-N removal efficiency exhibited a significantly positive correlation with $NO_3^-$-N concentration and $N_2O$ flux ($P < 0.05$), suggesting that the nitrification of $NH_4^+$-N might have been the primary contributor to the increase in $N_2O$ flux under varying water levels./

Fig. 4(f) depicts the relationship between moisture, nutrient removal and $N_2O$ emission in biochar-VFCWs. The study revealed a significant negative correlation between moisture and $NO_3^-$-N concentration ($P < 0.01$), suggesting that the increased moisture in biochar-VFCWs had enhanced the reduction of $NO_3^-$-N. Additionally, the $N_2O$/removed TN value was significantly negatively correlated with TN removal efficiency ($P < 0.05$), indicating that biochar effectively inhibited $N_2O$ emissions during the nitrogen cycling process. Furthermore, TN removal efficiency of biochar-VFCWs showed a significant positive correlation with $NH_4^+$-N removal efficiency ($P < 0.05$), highlighting that the nitrification process remained a limiting factor influencing overall nitrogen removal efficiency.

A comparative analysis revealed a significant positive correlation between water level and moisture in QS-CW (Fig. 4(e)), whereas this relationship was not significant with the addition

of biochar (Fig. 4(f)). This suggests that the combined effect of biochar and water level influenced water distribution in VFCWs. In the biochar-VFCWs, TN removal efficiency demonstrated a statistically significant negative correlation with the $N_2O$ /removed TN value ($P < 0.05$). In contrast, in the QS-CW, the $N_2O$ /removed TN value was positively correlated with TN removal efficiency. These findings indicate that biochar's better water holding capacity coupled with water level can simultaneously enhance nitrogen removal and reduce $N_2O$ emission.

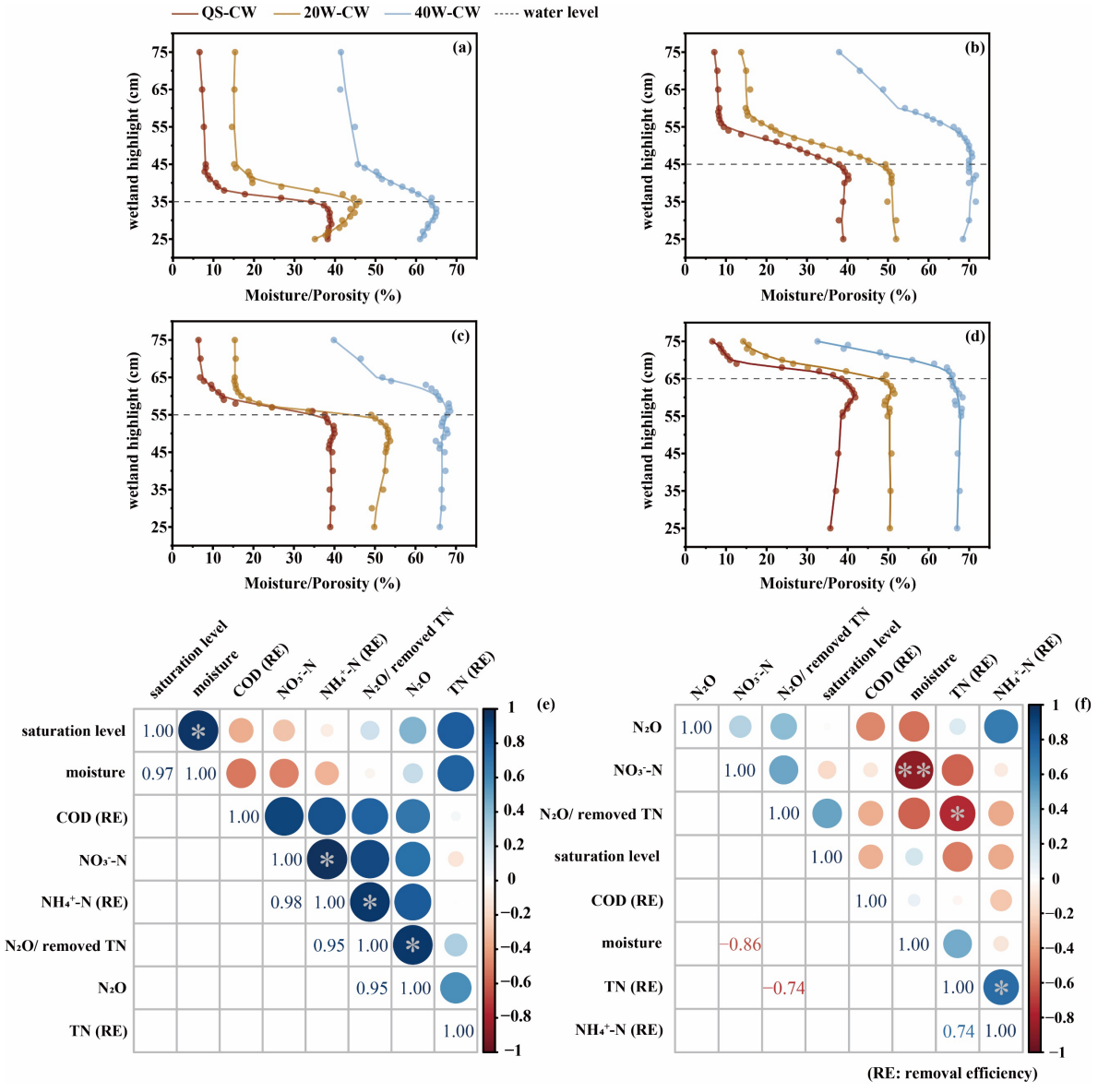



**Fig. 4.** The volume moisture (above water level) and porosity (below water level) of QS-CW, 20W-CW and 40W-CW at water level of 35 cm (a), 45 cm (b), 55 cm (c) and 65 cm (d), respectively. And effect of water level on moisture, nutrient removal and $N_2O$ emission of QS-CW (e) and biochar-VFCWs (f). * and ** represent significant correlations at $P < 0.05$ and $P < 0.01$, respectively.

### 3.3 Microbial ETS activity

The activity of the microbial extracellular electron transfer system of matrix microorganisms

in three parallel partially saturated VFCWs at a water level of 45 cm was studied. As shown in Fig. 5, the microbial ETS activity within the partially saturated VFCWs exhibited a decreasing trend along the wastewater flow.

For QS-CW, the ETS activity was ranked from high to low as follows: unsaturated zone (0.3 mg $O_2$ $g^{-1}{\cdot}h^{-1}$), capillary zone (0.04 mg $O_2$ $g^{-1}{\cdot}h^{-1}$), the saturated zone (0.01 mg $O_2$ $g^{-1}{\cdot}h^{-1}$). The abundant dissolved oxygen in the unsaturated zone was more conducive to enhancing ETS activity. Biochar effectively promoted the ETS activity of VFCWs, particularly in the capillary zone and saturated zone. ETS activity increased by 11.0%, 63.1%, and 266% for the unsaturated zone, capillary zone, and saturated zone of 20W-CW, respectively, similarly, 18.6%, 263% and 417% for 40W-CW of the three zones respectively, compared to QS-CW. These findings are consistent with those reported by Chen (Chen et al., 2023).

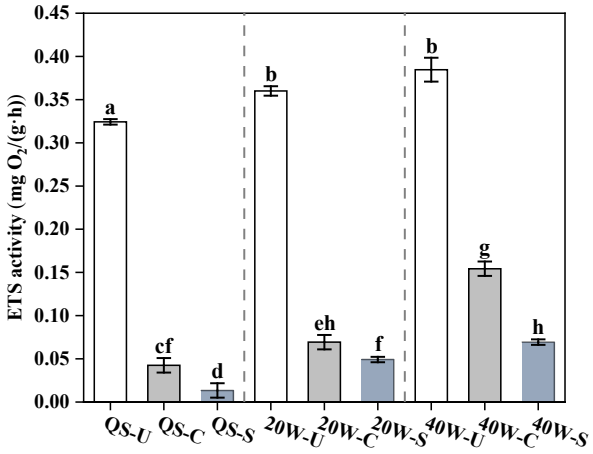



**Fig. 5.** ETS activity of microorganisms in unsaturated zone, capillary zone and saturated zone of VFCWs at water level of 45 cm. QS-CW-S, QS-CW-C, QS-CW-U, 20W-U, 20W-C, 20W-S, 40W-U, 40W-C, 40W-S represent unsaturated zone, capillary zone and saturated zone of QS-CW, 20W-CW and 40W-CW respectively. Different lowercase letters represent the significant difference among three VFCWs at $p < 0.05$ according to one-way ANOVA.

According to oxygen conduction characteristics in VFCWs, the aerobic zone was primarily distributed in the unsaturated zone, where aerobic metabolism of organic matter and nitrification reactions predominantly occurred. The anoxic/anaerobic environment was found in the capillary zone and saturated zone. 40W-CW exhibited higher ETS activity in unsaturated zone, capillary zone and saturated zone. The reason for this may be attributed to the porous structure of biochar, which was favor for capturing oxygen bubbles secreted by plant roots and atmospheric reoxygenation, thereby promoting extracellular electron transfer of microorganisms, accelerating nitrification, and resulted in the production of nitrate. The nitrate was then transported downwards, and the biochar present in the capillary and unsaturated zones served as electron donors for the denitrification process. Simultaneously, it functioned as an electron shuttle, enhancing electron transfer during denitrification. This ultimately facilitated nitrogen cycling process and suppressed $N_2O$ emission (Gu et al., 2023; Miao et al., 2024).

### 3.4 Distribution of functional microorganisms

With the addition of biochar, both the 20W-CW and 40W-CW systems exhibited a significant increase in Shannon, Chao, and Ace indices ($P < 0.05$), while the Simpson index decreased in the 20W-CW ($P < 0.05$) and 40W-CW systems. These results indicate that the addition of biochar significantly altered the microbial community composition within the constructed wetlands. The analysis of microbial alpha diversity revealed that the addition of biochar enhanced both species richness and evenness in the wetland substrate communities while reducing the dominance of certain species (Fig. 6(a)). This indicates that biochar amendment reduced the variability in microbial distribution and improved the stability of microbial communities in the constructed wetlands.

Fig. 6(b) illustrated the distribution of dominant microbial phyla in the unsaturated zone, capillary zone, and saturated zone of the three wetland systems. The dominant phyla include *Proteobacteria* (34.0%–50.5%), *Bacteroidetes* (6.1%–12.5%), *Planctomycetes* (4.5%–14.0%), *Chlamydiae* (0.8%–5.3%), *Acidobacteria* (2.3%–8.1%), *Verrucomicrobia* (2.0%–3.1%), *Nitrospirae* (0.2%–4.7%), *Chloroflexi* (0.4%–4.6%), *Actinobacteria* (1.4%–3.0%), and *Firmicutes* (0.7%–3.4%).

*Proteobacteria* emerged as the dominant phylum in all constructed wetlands, with its relative abundance decreasing as wetland depth increased in QS-CW. As the most abundant phylum, *Proteobacteria* accounted for 34.0%–50.5% of the total microbial community. Studies have shown that *Proteobacteria* are among the most typical bacteria involved in biological nitrogen removal, with many of its members being anaerobic or facultative anaerobic. Notably, bacteria within the *β-Proteobacteria* class can utilize organic matter as an electron donor, playing a critical role in completing the denitrification process (Singh et al., 2023; Zhang et al., 2024). As the sampling depth increased (from the unsaturated zone to the saturated zone), the relative abundance of *Proteobacteria* decrease. This phenomenon is attributed not only to the gradient of DO but also to the decreasing concentrations of organic matter and nitrogen in the influent wastewater. The reduced availability of organic carbon and nitrogen sources limits the energy supply required for the growth and metabolic activity of *Proteobacteria*, leading to a gradual decrease in their relative abundance. However, in 40W-CW, the relative abundance of Proteobacteria in the capillary zone (46.7%) was significantly higher than that in the unsaturated zone (43.3%) and saturated zone (35.3%). This could be attributed to the adsorption of organic matter, nitrogen of biochar, which provides an enriched nutrient supply for *Proteobacteria*. Additionally, the elevated moisture content in the capillary zone creates a favorable redox environment, further promoting microbial activity. These findings suggest that functional microorganisms in the capillary zone may play a dominant role in the nitrogen removal processes of constructed wetland, highlighting the critical influence of biochar and moisture conditions on microbial community dynamics and pollutant removal efficiency.

As a common phylum in wastewater treatment processes, *Bacteroidetes* are heterotrophic organisms involved in organic carbon cycling, capable of degrading proteins and producing various dissolved enzymes and acetate (Kong et al., 2022). However, with the addition of biochar, the relative abundance of *Bacteroidetes* in the unsaturated zone, capillary zone, and saturated zone of 20W-CW and 40W-CW decreased by 2.4%, 6.8%, 2.9% and 1.1%, 3.3%, 1.2%, respectively. Although the high proportion of biochar limited the oxidative environment in the substrate, the expanded habitat for functional microorganisms alleviated the constraints imposed by biochar on the growth of *Bacteroidetes*. This suggests that while biochar may initially restrict certain microbial groups, its overall impact on microbial diversity and functionality is balanced by the creation of a more favorable ecological niche for other functional microbes.

The main microbial genera involved in nitrogen cycling are shown in Fig. 6(c). Due to variations in the redox environment within the wetlands, the relative abundance of functional microbial genera in all constructed wetlands exhibited a consistent pattern with increasing depth: unsaturated zone > capillary zone > saturated zone. In unsaturated zone of 40W-CW, microorganisms that carried *amoA* and *hao* genes and involved in the oxidation process of $NH_4^+$-N to $NO_2^-$-N included *Nitrosomonas*, *Methylosarcina*, *Nitrosospira*, and *Methylomonas*. Their relative abundance was 0.08% higher than that of the QS-CW, representing a 75.2% increase. In 40W-CW, 64 genera that carried the *nxrB* gene, which was involved in the oxidation of $NO_2^-$-N to $NO_3^-$-N, were identified, whereas only 52 genera were found in the QS-CW system. The additional genera in 40W-CW include *Paracoccus*, *Cupriavidus*, et al. Furthermore, the diversity of functional genera that carried the *narG* gene, which was responsible for the reduction of $NO_3^-$-N to $NO_2^-$-N, also increased, including *Denitratisoma*, *Cupriavidus*, and *Pelagibacterium*.

This indicated that both nitrifying and denitrifying bacteria coexist in the unsaturated zone of the 40W-CW system. The addition of biochar not only enhanced the relative abundance of functional microorganisms and functional genes involved in the nitrification process, but also promoted the diversity of genera and the relative abundance of functional genes involved in $NO_3^-$-N reduction process. This extended the nitrogen cycling process, which was predominantly nitrification in the unsaturated zone, further into the denitrification process, creating a strong interweaving of nitrification and denitrification.

The *nosZ* gene encodes $N_2O$ reductase, a key enzyme responsible for catalysing the reduction of $N_2O$ to $N_2$, thereby facilitating the completion of the denitrification process. The relative abundance and expression of *nosZ* will influence the efficiency of $N_2O$ reduction, moreover, as the activity of *nosZ* enzyme is oxygen-sensitive, high oxygen environments inhibit its function. Consequently, the elevated moisture in the capillary zone reduces oxygen diffusion, leading to a significant increase in the abundance of the *nosZ* gene. In capillary zone of the

40W-CW, microorganisms carrying *nosZ* gene primarily included *Ferrovibrio* (0.6%), *Thauera* (0.4%), *Ramlibacter* (0.4%), and *Hyphomicrobium* (0.4%). In 40W-CW, the relative abundance of functional genera involved in $N_2O$ reduction (*Ferrovibrio*, *Thauera*, *Ramlibacter*, and *Hyphomicrobium* in the capillary zone increased by 1724%, 357%, 707%, and 78.5%, respectively, compared to QS-CW. The significant rise in the relative abundance of these functional genera suggests that biochar amendment enhances the microbial consumption of $N_2O$, indicating that the capillary zone of 40W-CW may serve as a potential consumption zone for $N_2O$. This finding underscores the stronger metabolic activity of functional microorganisms in the capillary zone of 40W-CW, driven by the favorable redox conditions and nutrient availability facilitated by biochar. Additionally, the ETS activity in the 40W-CW capillary zone was 72.5% higher than that in QS-CW (Fig. 5), which promoted the efficient expression of functional genes and facilitated the highly efficient reduction of $N_2O$ in the capillary zone (Louca et al., 2016b).

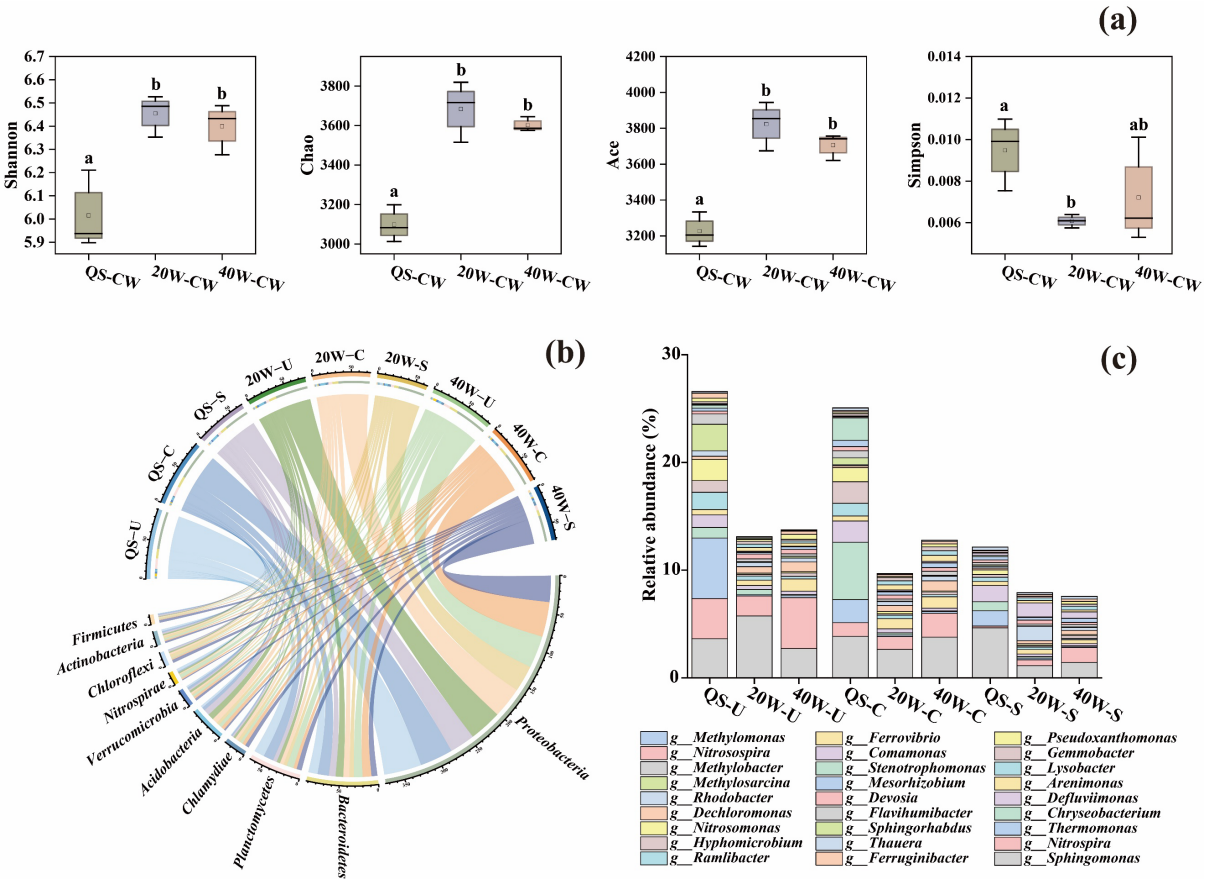



**Fig. 6.** Alpha diversity analysis of microorganisms in constructed wetlands (a); Distribution and composition of microorganisms at the phylum level across different depths in constructed wetlands (b); Relative abundance of key functional microorganisms involved in nitrogen transformation processes (carrying *amoA*, *hao*, *nxrB*, *narG*, *napA*, and *nosZ*) in the VFCWs (c).

In saturated zone of the 40W-CW, a significant presence of nitrifying genera carrying the *amoA* and *hao* genes was observed. Compared to the QS-CW system, the relative abundance of these functional genera increased by 0.04% (a 90.7% increase) and 0.2% (a 90.5% increase), respectively. This promoted the production and accumulation of $NO_2^-$-N. On the other hand, the relative abundance of microorganisms carrying the *nxrB* gene, such as *Methylosarcina*, *Actinomadura*, and *Enterovirga*, as well as the relative abundance of the *nxrB* gene, decreased by 20.0%. Higher relative abundance of microorganisms carrying the *amoA* and *hao* and lower relative abundance of microorganisms carrying the *nxrB* resulted in the accumulation of $NO_2^-$-N.

As shown in Table S4, the $NO_3^-$-N concentration in the effluent of 40W-CW decreased by 82.4% with the addition of biochar. In VFCWs, $NO_3^-$-N was the major nitrogen component in the effluent, while the amount of $NO_2^-$-N in the effluent was negligible. Limited carbon source (C/N=2:1) restricted denitrification in saturated zone of QS-CW. In 40W-CW, the population of ammonia-oxidizing bacteria increased, while the abundance of functional bacteria responsible for further oxidizing $NO_2^-$-N to $NO_3^-$-N decreased. It was hypothesized that the addition of biochar facilitates the reduction of accumulated $NO_2^-$-N through a carbon-efficient shortcut denitrification pathway (Hou et al., 2017), thereby ensuring an efficient denitrification process under low-carbon conditions.

### 3.5 Distribution of nitrogen cycling functional genes

The relative abundance of functional genes involved in nitrogen conversion processes of QS-CW, 20W-CW and 40W-CW were shown in Fig. 7. For nitrification process, *amoA*, *hao* and *nxrB* genes played key roles in converting $NH_4^+$-N to $NO_3^-$-N. In QS-CW, the average relative abundance of *amoA* and *hao* was 0.003% and 0.003%, respectively. This increased by 451% and 281% in 20W-CW, and by 702% and 286% in 40W-CW, respectively.

In QS-CW, the relative abundance of *amoA* in the unsaturated zone, capillary zone and saturated zone was 0.003%, 0.003% and 0.002%, respectively. Similarly, the relative abundance of *hao* was 0.003%, 0.003% and 0.002%, respectively. The study revealed that the abundance of *amoA* and *hao* genes in the unsaturated zone and capillary zone increased significantly in 20W-CW. In contrast, their abundance increased simultaneously across three zones in 40W-CW.

Additionally, the addition of biochar led to significant increase in the proportion of *amoA* and *hao* genes in saturated zone, with a 591% increase in *amoA* and a 149% increase in *hao*. It was previously reported that the nitrification process was the rate-limiting stage and played a crucial role in nitrogen purification efficiency (Wang et al., 2016). Therefore, the increase in the abundance of *amoA* and *hao* genes in 40W-CW enhanced the nitrification process, improved the removal efficiency of $NH_4^+$-N.

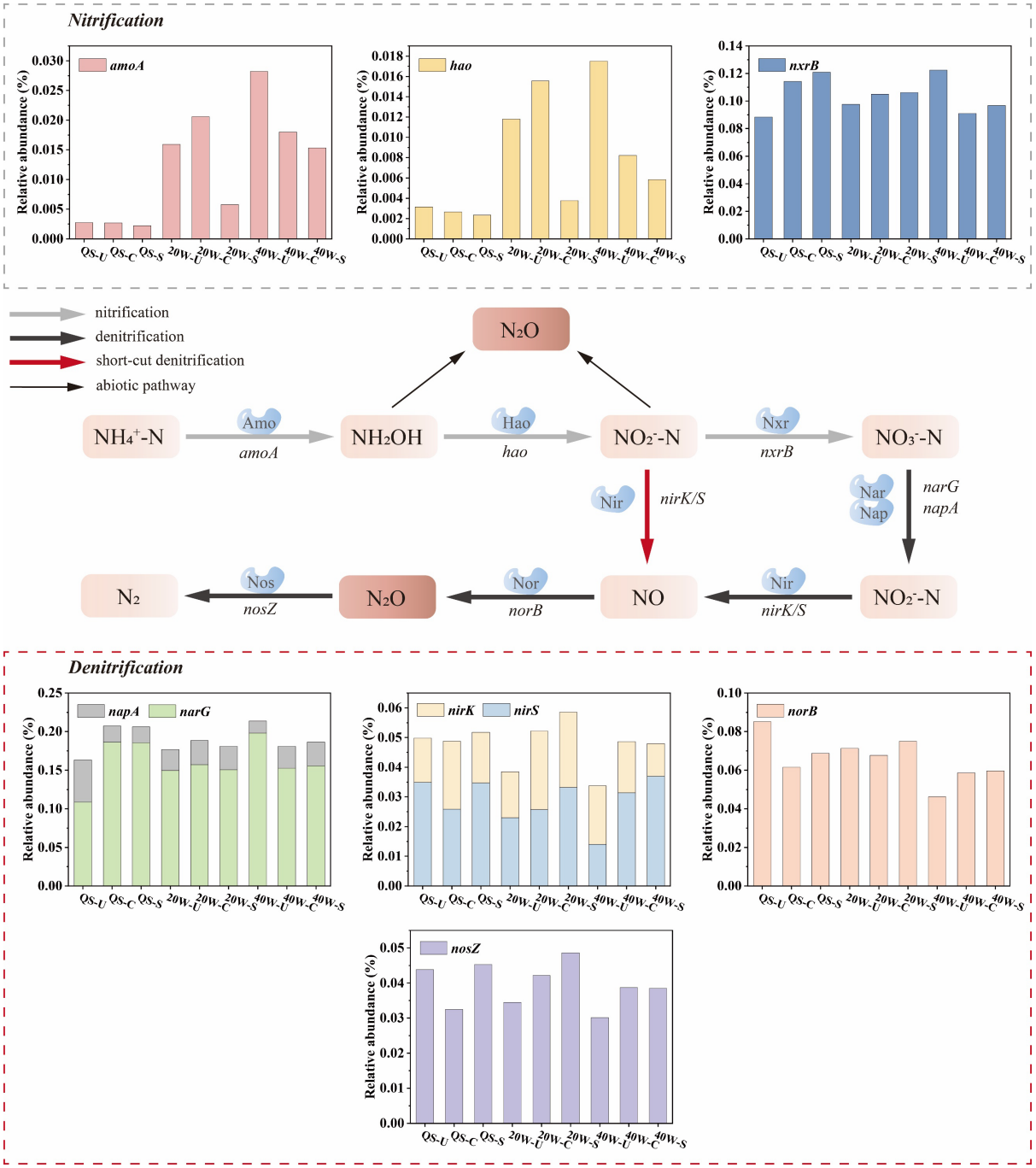



**Fig. 7.** Relative abundance of detected functional genes involved in nitrogen cycling at different sampling sites of nitrogen metabolism.

The relative abundance of *nxrB* in QS-CW and 20W-CW increased gradually cross unsaturated zone, capillary zone, and saturated zone, while it decreased gradually in 40W-CW. The relative abundance of *nxrB* in unsaturated zone of 40W-CW was 38.3% and 25.4% higher than that of QS-CW and 20W-CW, respectively. Indicating that the conversion of $NO_2^-$-N to $NO_3^-$-N by *nxrB* played a crucial role in preventing the accumulation of $NO_2^-$-N. Such efficient conversion was beneficial in reducing $N_2O$ production. On the other hand, the decrease in *nxrB* abundance of 40W-CW by 20.4% in the capillary zone and 20.0% in saturated zone, compared to QS-CW,

suggested a reduction in the intensity of $NO_2^-$-N conversion to $NO_3^-$-N. This reduction could potentially facilitate the direct denitrification process through the nitrite pathway, ultimately leading to higher nitrogen removal efficiency with low carbon source (Hou et al., 2017).

For denitrification, *napA*, *narG*, *nirK*, *nirS*, *norB*, and *nosZ* were known to played a crucial role in reduction of $NO_3^-$-N to $N_2$ (An et al., 2024). As illustrated in Fig. 6, *napA* and *narG*, which were responsible for the reduction of $NO_3^-$-N to $NO_2^-$-N in unsaturated zone of 40W-CW, exhibited a higher relative abundance compared to QS-CW and 20W-CW with increases of 30.8% and 20.9%, respectively. This suggested that more intense nitrification and denitrification had occurred in the unsaturated zone.

In QS-CW, the relative abundance of *nirKS* remained stable (0.05%) across all zones. However, in 20W-CW, *nirKS* exhibited a gradual increase from the unsaturated zone to saturated zone. Specifically, the relative abundance of *nirKS* in unsaturated zone differed from that in capillary zone by 2.1%, and the difference between the capillary zone and saturated zone was 6.1%. A similar pattern was observed in 40W-CW, where the relative abundance of *nirKS* between unsaturated zone and capillary zone increased by 44.3%.

Additionally, there were more anaerobic/aerobic denitrifying bacteria carrying *norB* in QS-S and 20W-S (13.4% and 25.8% higher than that in 40W-CW, respectively), which may promote $N_2O$ emissions.

The *nosZ* gene, which was involved in the reduction of $N_2O$ to $N_2$, was closely related to $N_2O$ emission (Pelissari et al., 2018; Zhang et al., 2023). The relative abundance of *nosZ* in unsaturated zone and saturated zone of 40W-CW was 31.3% and 15.1% lower than that of QS-CW, respectively. However, the relative abundance of *nosZ* in capillary zone was 19.2% higher than that of QS-CW, indicating an effective reduction of $N_2O$ in this zone. Based on this observation, it was speculated that the capillary zone might serve as a potential depletion layer for $N_2O$ in 40W-CW. Furthermore, as shown in Fig. 3(f), the $N_2O$/removed TN values for 40W-CW were notably lower than that of QS-CW at water level of 45 cm.

The higher relative abundance of *nosZ* in 20W-CW compared to 40W-CW could be attributed to the availability of reactants. As previously discussed, the addition of biochar had promoted the nitrification process and inhibited the emission of $N_2O$. Consequently, the lower $N_2O$ emission in 40W-CW resulted in fewer anaerobic/aerobic denitrifying bacteria carrying *nosZ*, which was involved in the reduction of $N_2O$ to $N_2$ in the unsaturated and saturated zones of 40W-CW.

Based on the analysis presented in Fig. 4, it was speculated that the elevation of microbial ETS activity in 40W-CW could be attributed to the amplified nitrification that facilitated by *amoA*, *hao*, *nxrB* and *narG* in the unsaturated zone, thereby significantly enhancing the removal of $NH_4^+$-N (Fig. 2). In addition, the increased ETS activity observed in the capillary zone of 40W-

CW might be the intensified denitrification facilitated by *nosZ*, subsequently reducing the generation of $N_2O$ (Fig.3).

It should be noted that although the number of functional genes involved in nitrogen cycling was similar between 40W-CW and QS-CW, the genus abundance of nitrogen-cycling bacteria in the 40W-CW system (11.4%) was lower than that in QS-CW (21.3%). This was primarily because the distribution and functional stability of these genes may be driven by a few key species or strains. In other words, despite a genus exhibiting high overall abundance, the functional gene abundance may remain low if only a limited proportion of bacterial strains possess the target functional genes (Louca et al., 2016a).

Based on the correlation analysis between functional genes, moisture, and ETS activity in QS-CW (Fig. 8(a)), moisture showed no significant correlation with functional genes involved in nitrogen transformation processes ($P > 0.05$). This indicates that the increase in moisture due to depth variation in the low-moisture substrate of QS-CW had no significant impact on nitrogen transformation processes in the absence of biochar. However, a significant positive correlation was observed between ETS activity and the relative abundance of *napA* (the genera carrying *napA* primarily include *Gemmobacter*, *Pseudoxanthomonas*, *Mesorhizobium*) ($P < 0.05$). Additionally, a significant negative correlation was found between the relative abundances of *napA* and *narG* (the genera carrying *narG* primarily include *Sphingomonas*, *Nitrospira*, *Defluviimonas*) ($P < 0.05$). These results suggest that regions with higher ETS activity in QS-CW at different depths contain more aerobic denitrification functional genes involved in nitrate reduction processes, highlighting the critical role of electron transport system activity in shaping microbial functional potential.

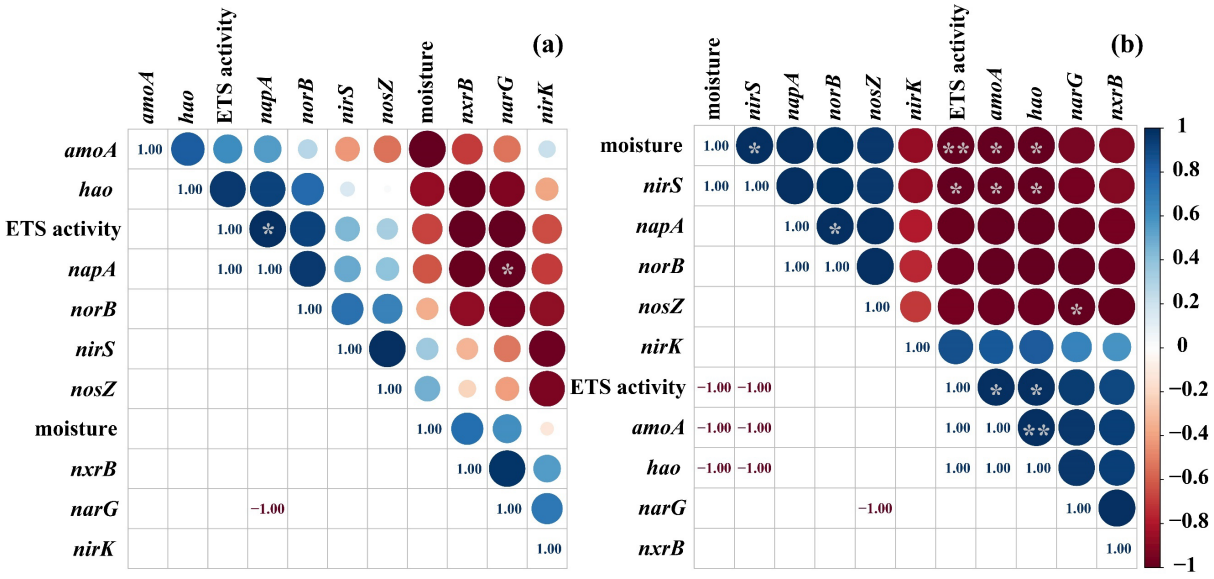



Fig. 8. Correlations among functional genes, moisture, and ETS activity in QS-CW (a) and 40W-CW (b). * and ** represent significant correlations at $P < 0.05$ and $P < 0.01$, respectively.

In 40W-CW (Fig. 8(b)), the high moisture content resulting from biochar addition significantly altered the distribution of functional genes involved in nitrogen transformation processes. The moisture in the 40W-CW substrate showed significant negative correlations with *amoA* (the genera carrying *amoA* primarily include *Methylosarcina*, *Methylobacter*) ($P < 0.05$), *hao* (the genera carrying *hao* primarily include *Nitrosomonas*, *Nitrosospira*) ($P < 0.05$), and ETS activity ($P < 0.01$). This indicates that the expression of *amoA* and hao is significantly influenced by moisture, and an increase in moisture markedly suppresses microbial activity in the substrate. Specifically, the rise in moisture in 40W-CW inhibited the expression of nitrification-related functional genes, such as *amoA*, *hao*, and *nxrB* (the genera carrying *nxrB* primarily include *Sphingomonas*, *Nitrospira*, *Lysobacter*), while promoting the expression of denitrification-related functional genes, such as *nirS* (the genera carrying *nirS* primarily include *Thermomonas*, *Defluviimonas*, *Arenimonas*), *napA*, and *norB* (the genera carrying *norB* primarily include *Sphingomonas*, *Thermomonas*, *Defluviimonas*). However, the impact of moisture on functional genes involved in nitrogen transformation was not significant in QS-CW, with weaker and less consistent correlations observed for genes associated with both nitrification and denitrification processes. These findings suggest that, compared to QS-CW, the expression of nitrification and denitrification functional genes in 40W-CW is more closely linked to moisture levels, leading to the formation of distinct functional zones dominated by either nitrification or denitrification processes.

### 3.5 Pollution reduction and $N_2O$ emission reduction mechanism of biochar

The microbiological mechanism of nitrogen cycling process for QS-CW and 40W-CW was shown in Fig. 9.

For QS-CW, 0.2% of TN was emitted in the form of $N_2O$, while 5.4% of TN was completely converted into $N_2$. The remaining 94.4% of TN existed as nitrate in the effluent of QS-CW. In 40W-CW, the proportion of $N_2O$ released in TN remained at 0.2%. However, the TN removed through complete microbial conversion to $N_2$ had increased to 73.2%, achieving a TN removal efficiency of 73.4% (67.8% higher than that of QS-CW). The $N_2O$/TN removal in 40W-CW and QS-CW were 0.3% and 3.9%, respectively. Notably, 40W-CW was 92.0% lower than QS-CW in terms of $N_2O$/TN removal. The biochar amendment partially saturated VFCWs effectively promoted nitrogen removal and reduced $N_2O$ emissions.

Better water holding capacity of biochar combined with regulated water levels, promoted the formation of nitrogen cycling microzones within CWs, creating a favourable ecological niche for microorganisms involved in nitrogen metabolism. Studies have shown that the nitrogen removal process requires spatial or temporal partitioning to produce a favourable ecological niche of aerobic nitrifying bacteria and anaerobic/anoxic denitrifying bacteria, so that functional genes could be efficiently co-expressed. This co-expression effectively inhibits $N_2O$ emission while improving nitrogen removal efficiency (Ruan et al., 2020). In this study, three

main reasons for the low $N_2O$/TN removal values observed in 40% biochar VFCW were as follows:

Firstly, biochar played a crucial role in facilitating a strong interweaving between nitrification and denitrification within the unsaturated zone.

The unsaturated zone was dominated by nitrification. With the addition of biochar, several high-moisture microzones formed, centered around the biochar. Which increased the retention time of pollutants in the unsaturated zone and enhanced mass transfer, significantly increasing the relative abundance of nitrification functional genes (92.9% for *amoA*), 454% for *hao* and 38.3% for *nxrB*. Moreover, the high water-holding capacity within these biochar-centered microzones effectively limited the diffusion of DO. Facilitated the denitrification process by microorganisms carrying *napA* and *narG*, extending the nitrogen cycle in the unsaturated zone from $NO_3^-$-N to $NO_2^-$-N, ultimately leading to a strong interweaving between nitrification and denitrification within the unsaturated zone.

Secondly, the addition of biochar made the capillary zone a potential depletion layer for $N_2O$.

The addition of biochar promoted *nosZ* in the capillary zone (increased by 19.2%), $N_2O$ discharged from the saturated zone and capillary zone could be captured by anaerobic/aerobic denitrifying bacteria carrying *nosZ* enriched in the capillary zone, $N_2O$ could be metabolized into $N_2$, and the production of $N_2O$ could also be reduced.

Thirdly, the addition of biochar promoted short-cut nitrification and denitrification process in saturated zone.

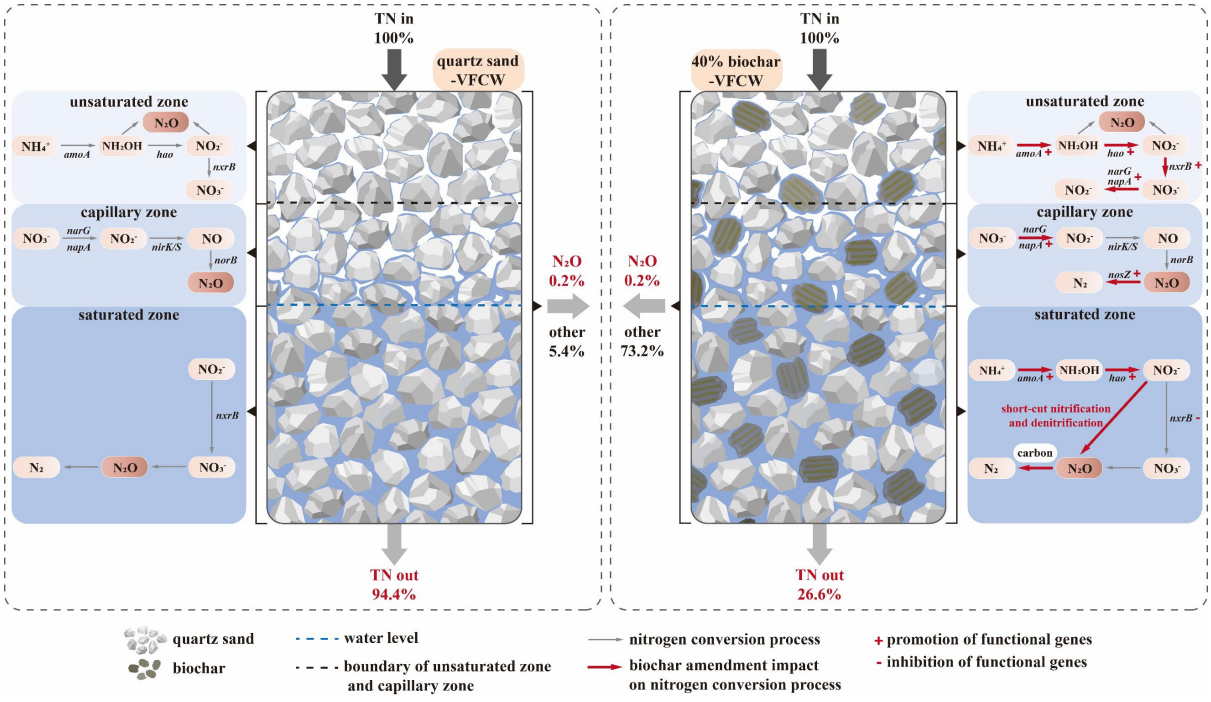



**Fig. 9.** Mechanism of biochar participating in $N_2O$ emission process.

Oxygen secreted by plant roots may be captured and stored by biochar and created a micro-aerobic environment, due to the porous structure, enhancing the relative abundance of *amoA* (increased by 591%) and *hao* (increased by 149%) in saturated zone, thereby promoting the oxidation of $NH_4^+$-N to $NO_2^-$-N. However, ammonium oxidizing bacteria exhibited a higher affinity for oxygen than nitrate oxidizing bacteria. Ammonia oxidizing bacteria carrying *amoA* and *hao* preferentially consumed DO, limiting the growth of nitrite oxidizing bacteria carrying *nxrB* (reduced by 20.0%) (Hou et al., 2017). The accumulated $NO_2^-$-N promoted direct conduct of denitrification process through the nitrite pathway.

## 4. Conclusion

This study demonstrated that coupling of 40% biochar and water level of 45 cm in partially saturated VFCWs significantly increased the ETS activity, achieving a high TN removal efficiency of 73.4% and a low $N_2O$/TN removal ratio of 0.3%. The addition of 40% biochar increased the relative abundance of the *amoA* and *hao* genes in constructed wetlands by 702% and 286%, respectively, improved nitrification throughout the entire bed and promoted short-cut nitrification and denitrification processes in the saturated zone. At the same time, it facilitated the proliferation of denitrifying bacteria such as *Ferrovibrio*, *Thauera*, *Ramlibacter* and *Hyphomicrobium*, which carry *nosZ* in the capillary zone, potentially forming a depletion layer for $N_2O$. The $N_2O$ produced in the saturated zone could be further reduced to $N_2$ in the capillary zone, thereby improving nitrogen removal efficiency and reducing $N_2O$ emission.

**CRediT Author Statement**

**Xin Wang**: Writing – original draft, Software, Visualization. **Zhiqiang Shen**: Methodology, Validation. **Qin Zhang**: Investigation, Data curation. **Tao Lyu**: Writing – review & editing. **Yanli Ding**: Formal analysis. **Shaoyuan Bai**: Conceptualization, Project administration, Resources, Supervision, Funding acquisition.

**Declaration of Competing Interest**

The authors declare that they have no known competing financial interests or personal relationships that could have appeared to influence the work reported in this paper.

**Acknowledgments**

This research is financially supported by the National Natural Science Foundation of China (52260024), the Guangxi Key Research and Development Program (Guike AB22080067), and the National Natural Science Foundation of China ( 52360024).

**Data availability**

Data will be made available on request.

## Reference


An, Z. et al., 2024. Synchronous Achievement of Advanced Nitrogen Removal and $N_2O$ Reduction in the Anoxic Zone in the AOA Process for Low C/N Municipal Wastewater. Environmental Science & Technology. 58 (5), 2335-2345. https://doi.org/10.1021/acs.est.3c06746

Banerjee, S. et al., 2016. Legacy effects of soil moisture on microbial community structure and $N_2O$ emissions. Soil Biology & Biochemistry. 95, 40-50. https://doi.org/10.1016/j.soilbio.2015.12.004

Cayuela, M.L. et al., 2014. Biochar's role in mitigating soil nitrous oxide emissions: A review and meta-analysis. Agriculture Ecosystems & Environment. 191, 5-16. https://doi.org/10.1016/j.agee.2013.10.009

Chen, X. et al., 2020. Greenhouse gas emissions and wastewater treatment performance by three plant species in subsurface flow constructed wetland mesocosms. Chemosphere. 239, 124795. https://doi.org/10.1016/j.chemosphere.2019.124795

Chen, Y. et al., 2023. Varied promotion effects and mechanisms of biochar on anaerobic digestion (AD) under distinct food-to-microorganism (F/M) ratios and biochar dosages. Waste Management. 155, 118-128. https://doi.org/10.1016/j.wasman.2022.10.030

Edeh, I.G. and Mašek, O., 2021. The role of biochar particle size and hydrophobicity in improving soil hydraulic properties. European Journal of Soil Science. 73 (1), 183-191. https://doi.org/10.1111/ejss.13138

Feng, L. et al., 2020. Can biochar application improve nitrogen removal in constructed wetlands for treating anaerobically-digested swine wastewater? Chemical Engineering Journal. 379, 122273. https://doi.org/10.1016/j.cej.2019.122273

Foltz, M.E. et al., 2019. Prediction of $N_2O$ emissions under different field management practices and climate conditions. Science of the Total Environment. 646, 872-879. https://doi.org/10.1016/j.scitotenv.2018.07.364

Gu, Y. et al., 2023. Optimization and control strategies of aeration in WWTPs: A review. Journal of Cleaner Production. 418, 138008. https://doi.org/https://doi.org/10.1016/j.jclepro.2023.138008

Guo, F. et al., 2020. Impact of biochar on greenhouse gas emissions from constructed wetlands under various influent chemical oxygen demand to nitrogen ratios. Bioresource Technology. 303, 122908. https://doi.org/10.1016/j.biortech.2020.122908

Hou, J. et al., 2017. Achieving short-cut nitrification and denitrification in modified intermittently aerated constructed wetland. Bioresource Technology. 232, 10-17. https://doi.org/https://doi.org/10.1016/j.biortech.2017.02.027

Huang, L. et al., 2012. A review on the mechanism and affecting factors of nitrous oxide emission in constructed wetlands. Environmental Earth Sciences. 68 (8), 2171-2180. https://doi.org/10.1007/s12665-012-1900-z

Huang, L. et al., 2023. Pathways and biological mechanisms of $N_2O$ emission reduction by adding biochar in the constructed wetland based on $^{15}N$ stable isotope tracing. Journal of Environmental Management. 342, 118359. https://doi.org/10.1016/j.jenvman.2023.118359

Huo, J. et al., 2022. Effects and mechanisms of constructed wetlands with different substrates on $N_2O$ emission in wastewater treatment. Environmental Science and Pollution Research. 29 (13), 19045-19053. https://doi.org/10.1007/s11356-021-17219-6

Kong, Z. et al., 2022. Unveiling the characterization and development of prokaryotic community during the start-

up and long-term operation of a pilot-scale anaerobic membrane bioreactor for the treatment of real municipal wastewater. Science of the Total Environment. 813, 152643. https://doi.org/https://doi.org/10.1016/j.scitotenv.2021.152643

Li, J. et al., 2019. Enhanced nitrogen removal in biochar-added surface flow constructed wetlands: dealing with seasonal variation in the north China. Environmental Science and Pollution Research. 26 (4), 3675-3684. https://doi.org/10.1007/s11356-018-3895-9

Li, X. et al., 2018. Effects of rice-husk biochar on sand-based rootzone amendment and creeping bentgrass growth. Urban Forestry & Urban Greening. 35, 165-173. https://doi.org/10.1016/j.ufug.2018.09.001

Liang, Y. et al., 2020. Insight into the mechanisms of biochar addition on pollutant removal enhancement and nitrous oxide emission reduction in subsurface flow constructed wetlands: Microbial community structure, functional genes and enzyme activity. Bioresource Technology. 307, 123249. https://doi.org/10.1016/j.biortech.2020.123249

Louca, S. et al., 2016a. High taxonomic variability despite stable functional structure across microbial communities. Nature Ecology & Evolution. 1 (1), 0015. https://doi.org/10.1038/s41559-016-0015

Louca, S. et al., 2016b. Decoupling function and taxonomy in the global ocean microbiome. Science. 353 (6305), 1272-1277. https://doi.org/10.1126/science.aaf4507

Lu, S. et al., 2019. Assessment of the treatment of domestic sewage by a vertical-flow artificial wetland at different operating water levels. Journal of Cleaner Production. 208, 649-655. https://doi.org/10.1016/j.jclepro.2018.10.111

Mekala, C. and Nambi, I.M., 2017. Understanding the hydrologic control of N cycle: Effect of water filled pore space on heterotrophic nitrification, denitrification and dissimilatory nitrate reduction to ammonium mechanisms in unsaturated soils. Journal of Contaminant Hydrology. 202, 11-22. https://doi.org/10.1016/j.jconhyd.2017.04.005

Miao, X. et al., 2024. Indigenous mixotrophic aerobic denitrifiers stimulated by oxygen micro/nanobubble-loaded microporous biochar. Bioresource Technology. 391, 129997. https://doi.org/https://doi.org/10.1016/j.biortech.2023.129997

Pelissari, C. et al., 2018. Effects of partially saturated conditions on the metabolically active microbiome and on nitrogen removal in vertical subsurface flow constructed wetlands. Water Research. 141, 185-195. https://doi.org/10.1016/j.watres.2018.05.002

Ruan, Y. et al., 2020. Kinetic affinity index informs the divisions of nitrate flux in aerobic denitrification. Bioresource Technology. 309, 123345. https://doi.org/https://doi.org/10.1016/j.biortech.2020.123345

Saeed, T. et al., 2019. Organic matter and nutrients removal in hybrid constructed wetlands: Influence of saturation. Chemical Engineering Journal. 371, 154-165. https://doi.org/10.1016/j.cej.2019.04.030

Saquing, J.M. et al., 2016. Wood-Derived Black Carbon (Biochar) as a Microbial Electron Donor and Acceptor. Environmental Science & Technology Letters. 3 (2), 62-66. https://doi.org/10.1021/acs.estlett.5b00354

Singh, S. et al., 2022. Customized design of horizontal flow constructed wetlands employing secondary datasets. Bioresource Technology Reports. 18, 101037. https://doi.org/https://doi.org/10.1016/j.biteb.2022.101037

Singh, S. et al., 2023. Optimization of depth of filler media in horizontal flow constructed wetlands for maximizing removal rate coefficients of targeted pollutant(s). Bioresource Technology. 376, 128898. https://doi.org/https://doi.org/10.1016/j.biortech.2023.128898

Singh, S. et al., 2024b. Machine Learning Application for Nutrient Removal Rate Coefficient Analyses in Horizontal Flow Constructed Wetlands. ACS ES&T Water. 4 (6), 2619-2631. https://doi.org/10.1021/acsestwater.4c00121

836 Singh, S. et al., 2024a. A Futuristic Approach to Subsurface-Constructed Wetland Design for the South-East Asian
837 Region Using Machine Learning. ACS ES&T Water. 4 (9), 4061-4074.
838 https://doi.org/10.1021/acsestwater.4c00346
839 Soti, A. et al., 2024. High rates of nitrogen removal in aerated VFCWs treating sewage through C-N-S cycle.
840 Bioresource Technology. 399, 130620. https://doi.org/https://doi.org/10.1016/j.biortech.2024.130620
841 Vicente, I.d. et al., 2010. Contrasting factors controlling microbial respiratory activity in the sediment of two
842 adjacent Mediterranean wetlands. Naturwissenschaften. 97 (7), 627-635.
843 https://doi.org/10.1007/s00114-010-0678-7
844 Vymazal, J., 2013. The use of hybrid constructed wetlands for wastewater treatment with special attention to
845 nitrogen removal: A review of a recent development. Water Research. 47 (14), 4795-4811.
846 https://doi.org/10.1016/j.watres.2013.05.029
847 Vymazal, J. and Dvořáková Březinová, T., 2018. Treatment of a small stream impacted by agricultural drainage in
848 a semi-constructed wetland. Science of the Total Environment. 643, 52-62.
849 https://doi.org/10.1016/j.scitotenv.2018.06.148
850 Wang, B. et al., 2016. Impact of partial nitritation degree and C/N ratio on simultaneous Sludge Fermentation,
851 Denitrification and Anammox process. Bioresource Technology. 219, 411-419.
852 https://doi.org/10.1016/j.biortech.2016.07.114
853 Wang, D. et al., 2019. Impact of biochar on water retention of two agricultural soils – A multi-scale analysis.
854 Geoderma. 340, 185-191. https://doi.org/10.1016/j.geoderma.2019.01.012
855 Wang, J. et al., 2023. Efficient removal mechanism of an electrical conductivity-enhanced constructed wetlands
856 under particle accumulated conditions. Journal of Cleaner Production. 411.
857 https://doi.org/10.1016/j.jclepro.2023.137257
858 Wu, H. et al., 2023. Constructed wetlands for pollution control. Nature Reviews Earth & Environment. 4 (4), 218-
859 234. https://doi.org/10.1038/s43017-023-00395-z
860 Yang, H.I. et al., 2018. Adsorption of ammonium in aqueous solutions by pine sawdust and wheat straw biochars.
861 Environmental Science and Pollution Research. 25 (26), 25638-25647. https://doi.org/10.1007/s11356-
862 017-8551-2
863 Yao, Y. et al., 2019. Modeling capillary fringe effect on petroleum vapor intrusion from groundwater
864 contamination. Water Research. 150, 111-119.
865 https://doi.org/https://doi.org/10.1016/j.watres.2018.11.038
866 Yi, S. et al., 2020. Predicting water retention of biochar-amended soil from independent measurements of
867 biochar and soil properties. Advances in Water Resources. 142, 103638.
868 https://doi.org/10.1016/j.advwatres.2020.103638
869 Yin, Q. et al., 2018. Clarifying electron transfer and metagenomic analysis of microbial community in the methane
870 production process with the addition of ferroferric oxide. Chemical Engineering Journal. 333, 216-225.
871 https://doi.org/10.1016/j.cej.2017.09.160
872 Zhang, L. et al., 2023. Unveiling the nitrogen removal performance from microbial network establishment in
873 vertical flow constructed wetlands. Bioresource Technology. 388, 129749.
874 https://doi.org/https://doi.org/10.1016/j.biortech.2023.129749
875 Zhang, S. et al., 2024. Efficient nitrogen removal by multi-stage A/O mud membrane composite process with
876 segmented influent: Performance and microbial community structure. Environmental Research. 250,
877 118446. https://doi.org/https://doi.org/10.1016/j.envres.2024.118446
878 Zhang, X. et al., 2018. Autotrophic and heterotrophic nitrification-anoxic denitrification dominated the
879 anoxic/oxic sewage treatment process during optimization for higher loading rate and energy savings.

Bioresource Technology. 263, 84-93. https://doi.org/https://doi.org/10.1016/j.biortech.2018.04.113

Zhao, Y.-J. et al., 2013. Performance of hybrid vertical up- and downflow subsurface flow constructed wetlands in treating synthetic high-strength wastewater. Environmental Science and Pollution Research. 20 (7), 4886-4894. https://doi.org/10.1007/s11356-013-1467-6

Zheng, F. et al., 2022. Biochar based constructed wetland for secondary effluent treatment: Waste resource utilization. Chemical Engineering Journal. 432, 134377. https://doi.org/10.1016/j.cej.2021.134377

Zhou, X. et al., 2018. Simultaneous enhancement of nitrogen removal and nitrous oxide reduction by a saturated biochar-based intermittent aeration vertical flow constructed wetland: Effects of influent strength. Chemical Engineering Journal. 334, 1842-1850. https://doi.org/10.1016/j.cej.2017.11.066

Zhou, X. et al., 2017. Enhanced nitrogen removal of low C/N domestic wastewater using a biochar-amended aerated vertical flow constructed wetland. Bioresource Technology. 241, 269-275. https://doi.org/10.1016/j.biortech.2017.05.072

https://dspace.org/

# Biochar amendment and water level optimization enhance nitrogen removal and reduce N2O emissions in vertical flow constructed wetlands via metagenomic analysis

**Wang, Xin; Shen, Zhiqiang; Zhang, Qin; Lyu, Tao; Ding, Yanli ...**

**2025-08**
Elsevier
https://doi.org/10.1016/j.jenvman.2025.126133
Wang X, Shen Z, Zhang Q, et al., (2025) Biochar amendment and water level optimization enhance nitrogen removal and reduce N2O emissions in vertical flow constructed wetlands via metagenomic analysis. Journal of Environmental Management, Volume 389, August 2025, Article number 126133

Downloaded from a DSpace repository. https://dspace.org/